Electronic Supplementary Material (ESI) for ChemComm.

Effect of pH on chitosan hydrogel polymer network structure

Hongcheng Xu[†] and Silvina Matysiak[*,†,‡]

Biophysics Program, Institute of Physical Science and Technology, University of Maryland, College Park, MD, and Fischell Department of Bioengineering, University of Maryland, College Park, MD

E-mail: matysiak@umd.edu

[*]To whom correspondence should be addressed

[†]Biophysics Program, Institute of Physical Science and Technology, University of Maryland, College Park, MD

[‡]Fischell Department of Bioengineering, University of Maryland, College Park, MD

Methods

CG Model

In our mapping scheme, we approximately group 4 heavy atoms into a single coarse-grained bead. As shown in Figure 1, the B1 bead includes atoms from the hydroxyl side chain, the B2 bead includes most of the polymer backbone atoms, and the B3 bead maps the hydroxyl and amino groups opposite to the B1 side chain. All three beads have different levels of hydrophilicity, and the B3 bead can become protonated depending on the pH. The basic bead type used in our chitosan model is taken from the MARTINI carbohydrates coarse-grained force field parameter set,[1] in which each building block is categorized as apolar, polar or charged. The polarity types of B1, B2 and B3 beads are in increasing order, and B3 bead becomes positively charged in an acidic environment. The polarity is determined by comparing to oligosaccharides examples provided in the MARTINI CG model for carbohydrates.[1] Each chitosan chain is designed to have 10 monomers so that the total length is within the experimentally reported persistence length (5-15nm).[2–5]

Table S1: Bond, angle and dihedral parameters.

bonds	R_{bond} (nm)	K_{bond} (kJ mol^{-1} nm^{-2})
B1-B2	0.2494	30000
B2-B3	0.1934	30000
B2-B2'	0.5211	30000
angles	$\theta_0(deg)$	K$_{angle}$ (kJ mol^{-1})
B1-B2-B3	123.76	450
B2-B2'-B2"	163.78	350
B2-B2'-B1'	70.94	450
B1-B2-B2'	90.88	100
B3-B2-B2'	135.94	300
B3'-B2'-B2	58.01	800
dihedrals	$\psi_{pd}(deg)$	K$_{pd}$ (kJ mol^{-1})
B1-B2-B2'-B1'	175.62	8
B1-B2-B2'-B3'	-28.59	10
B3-B2-B2'-B1'	36.57	18

The force field (see Eq. 1) consists of bonded interactions (harmonic bonded, angular potential and proper dihedral, see Table S1) and non-bonded interactions (12-6 Lennard-

Table S2: Non-bonded Lennard-Jones (LJ) interaction strengths. Unit of interaction strength (ϵ) is in kJ/mol. The radius (σ) of all LJ interactions is 4.7Å.

Beads	B1	B2	B3	$B3^+/Cl^-$	Water
B1	5.0	5.0	5.6	5.6	4.75
B2	5.0	5.0	5.6	5.6	4.75
B3	5.6	5.6	5.6	5.6	5.32
$B3^+/Cl^-$	5.6	5.6	5.6	3.5	5.0
Water	4.75	4.75	5.32	5.0	4.0

Jones potential and Coulombic potential, see Table S2). The bonded interaction parameters are tuned from fitting the distributions of corresponding bonds, angles and dihedrals to atomistic simulation results using GROMOS 53A6GLYC force field.[6] CG bond and angle distributions match well with corresponding distributions in atomistic simulation as shown in Figure S1. Non-bonded interactions are defined according to bead type definitions in the MARTINI CG force field (extension to carbohydrates).[1] The most polar bead, B3, is defined as comparable to a building block of acetamide because of the presence of the amino group in the bead. The less polar B1 and B2 beads are defined as similar polarity as propanol and ethanol. The protonated B3 bead ($B3^+$) is defined similarly to protonated propylamine. In addition, the torsional angles ϕ_{CG}, ψ_{CG} (as defined in Figure S2b) distribution map of chitosan chains for atomistic (Figure S2c) and CG (Figure S2d) models sample similar configurations in both models. The atomistic model samples the 2-fold helical conformation since the values of ψ and ϕ are centered in the ψ and ϕ of 2-fold helix ($\phi \cong -98°$, $\psi \cong 92°$ in Figure S2a).[7] Therefore, the conformation of CG chitosan polymers in the simulation resembles the 2-fold helix most commonly observed experimentally.[8–11] In the atomistic simulation, the scale of the simulation box is limited (see simulation setup). Since the box size is limited for performance, to simulate an infinite chitosan chain, both ends of a single-chained chitosan polymer are connected through the periodic boundary box. With the exclusion 1-2, 1-3, 1-4 non-bonded interactions, the proper dihedrals are used to reproduce the secondary structure in the atomistic chitosan simulations. The MARTINI polarizable CG water[12] model is used as it is needed to achieve the right behavior of chitosan self-assembly

under low pH. The usage of non-polarizable MARTINI CG water results in overbinding of anionic ions to protonated chitosan polymers, leading to chain condensation at low pH.

$$U_{\text{total}} = U_{\text{bonded}} + U_{\text{non-bonded}}, \tag{1a}$$

$$U_{\text{bonded}} = U_{\text{bonds}} + U_{\text{angles}} + U_{\text{dihedrals}}, \tag{1b}$$

$$U_{\text{non-bonded}} = U_{\text{vdW}} + U_{\text{electrostatics}}, \tag{1c}$$

$$U_{\text{bonds}} = \sum_{bonds} \frac{1}{2} k_l (l - l_0)^2, \tag{1d}$$

$$U_{\text{angles}} = \sum_{angles} \frac{1}{2} k_\theta (\theta - \theta_0)^2, \tag{1e}$$

$$U_{\text{dihedral}} = \sum_{dihedrals} k_\phi (1 + \cos(n\phi - \phi_0)), \tag{1f}$$

$$U_{\text{vdW}} = \sum_{pairs(i \neq j)} 4\epsilon_{ij} \left[\left(\frac{\sigma}{r} \right)^{12} - \left(\frac{\sigma}{r} \right)^{6} \right], \tag{1g}$$

$$U_{\text{electrostatics}} = \sum_{pairs(i \neq j)} \frac{q_{\text{i}} q_{\text{j}}}{4\pi\epsilon_0 \epsilon_{\text{r}} r}, \tag{1h}$$

Simulation Parameters and Setup

Atomistic simulation

The atomistic simulation was set up with GROMOS53A6 force field.[6] In the simulation, a single 10-mer chitosan polymer chain was connected through the periodic boundary to create an infinite chain. The length of the polymer chain was set to around 5 nm, to capture the minimal persistence lengths reported in experiments.[2,3] In the simulation, 1445 SPC water molecules were used to solvate the chitosan chain. The timestep of atomistic simulation was 1 fs, and the simulation integration method was leapfrog.[13] The total length of the isothermal-isobaric (NPT) simulation was 100 ns, and the last 10 ns was used for analysis. Berendsen

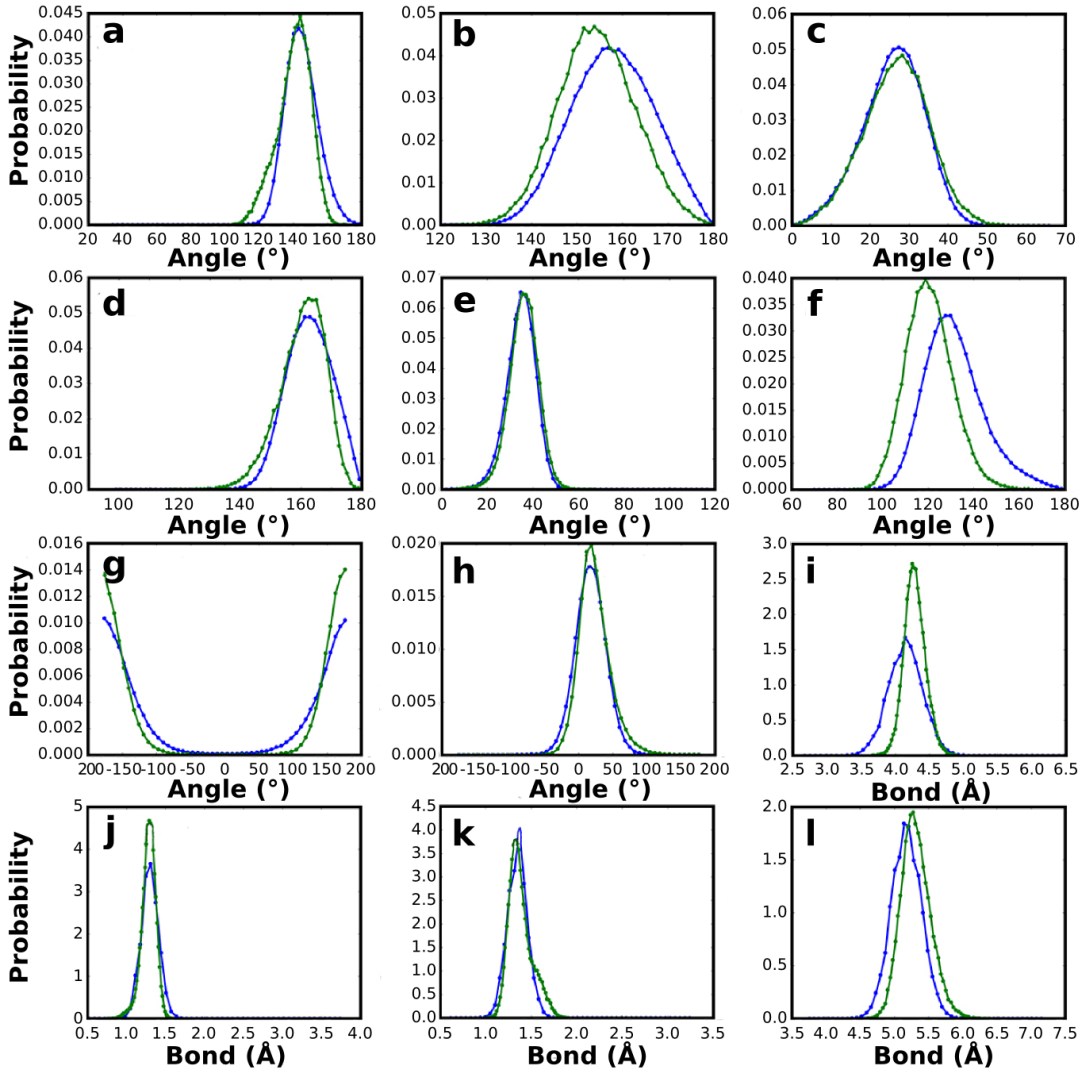

Figure S1: Bond and angle distribution comparison in atomistic (green) and CG simulations (blue). (a) B1-B2-B3 angle; (b) backbone angle formed by 3 consecutive backbone B2 beads (B2-B2'-B2"); (c) B2-B2'-B1' angle; (d) B1-B2-B2' angle; (e) B3-B2-B2' angle; (f) B2-B2'-B3 angle; (g) backbone dihedral angle formed by 4 consecutive backbone B2 beads (B2-B2'-B2"-B2"'); (h) B3-B2-B2'-B1' dihedral angle; (i) B3-B2' bond; (j) B1-B2 bond; (k) B2-B3 bond; (l) B2-B2' bond.

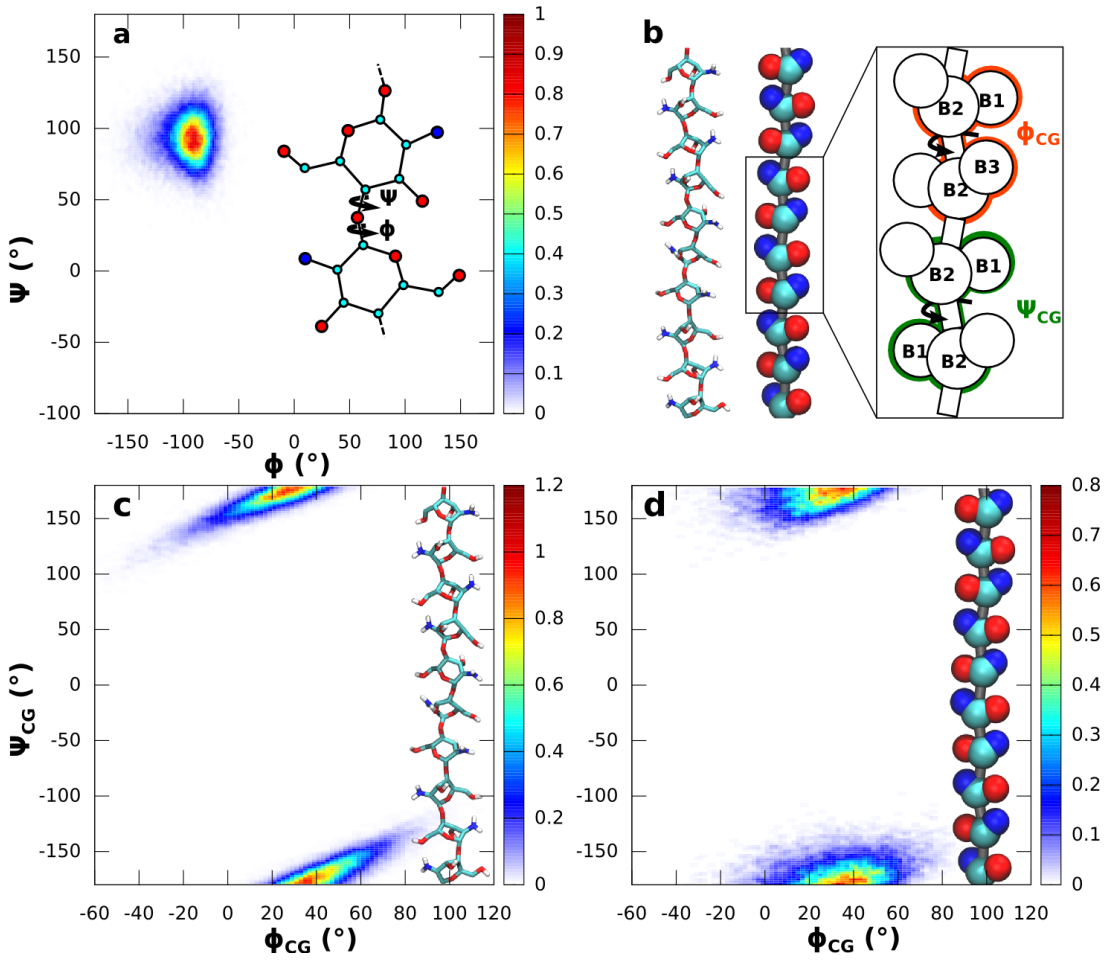

Figure S2: Extended 2-fold helix conformation of chitosan chains in atomistic and CG models. (a) ϕ and ψ torsional angle distribution map of a chitosan chain in atomistic simulation; (b) Chitosan chains with extended 2-fold helical conformations in atomistic model (left) and CG model (center). Chitosan CG model is zoomed in to show definitions of CG torsional angles ϕ_{CG} and ψ_{CG}; ϕ_{CG} is defined as the torsional angle formed by B1, B2 beads in one monomer and B2, B1 beads in the subsequent monomer, and ψ_{CG} is defined as the torsional angle formed by B3, B2 beads in one monomer and B2, B1 beads in the subsequent monomer; (c) Torsional angle distribution map of chitosan in atomistic model; (d) Torsional angle distribution map of chitosan in CG model.

temperature and pressure coupling schemes[14] were used with a reference temperature of 300 K, and pressure of 1 atm. The relaxation time of the temperature coupling was 0.1 ps and of the pressure coupling was 1.0 ps. Semi-isotropic pressure coupling was used in the simulation with a compressibility of 4.5×10^{-5} bar^{-1}. Coulombic interactions were treated with the generalized reaction field method[15] with $\epsilon = 66$. A 1.4 nm cutoff distance was used for the short-range electrostatics and van der Waals interactions.

CG simulations with GROMACS

Coarse-grained simulations were set up using our model. 50 ns isothermal-isobaric (NPT) simulations were run after 10 ns of randomization simulations. In the randomization process, all chitosan beads were set to slightly repel each other so that polymer chains can disperse and fill the entire simulation box. The last 10 ns of NPT data was used for analysis. The timestep of the CG simulations was 20 fs, and the simulation integrator was leapfrog.[13] Nose-Hoover temperature coupling[16,17] and Parrinello-Rahman pressure coupling schemes[18] were used with a reference temperature of 300 K, and pressure of 1 atm. The relaxation time of the temperature coupling was 1 ps and of the pressure coupling was 10 ps. Isotropic pressure coupling was used in the simulation with a compressibility of 4.5×10^{-6} bar^{-1}. Coulombic interactions were treated with particle-mesh Ewald method[19,20] with $\epsilon = 2.5$. A 1.6 nm cutoff distance was used for the short-range electrostatics and van der Waals interactions. The constraint algorithm LINCS was used to constrain the MARTINI polarizable water dummy bonds[21] (For details of MARTINI polarizable water model, see Ref[12]).

12 simulations were set up with different water contents and pH. Water content was modeled by changing concentrations of chitosan polymer chains in the simulation box. 20, 40, 60, and 80 chitosan 30-mer polymer chains were randomly put into the simulation box and solvated with around 37000 polarizable MARTINI water beads corresponding to water contents of 95.4%, 91.1%, 86.4%, and 82.3% respectively. Solution pH was modeled by changing the percentage of protonated chitosan B3 bead using the Henderson-Hasselbalch

equation. 0%, 50%, and 100% of chitosan B3 side chain beads were randomly protonated corresponding to pH of >10.5 (<0.01% protonation), 6.5 (∼50% protonation, pKa≃ 6.5), and <2.5 (>99.99% protonation) respectively.

CG simulations with LAMMPS

We transferred the simulations from GROMACS to LAMMPS so that we could deform the box size in the simulation to measure the elastic moduli of chitosan hydrogels. The same sets of water contents and pH combinations were used as in the GROMACS NPT simulations. LAMMPS CG simulations were set up using our model. The initial conformation was taken from the last frame of 50 ns GROMACS NPT runs. The timestep of the CG simulation was 20 fs, and the simulation integrator was velocity-Verlet.[22] Nose-Hoover temperature coupling[16,17] and Parrinello-Rahman pressure coupling schemes[18] were used with a reference temperature of 300 K, and pressure of 1 atm. The damping parameter of temperature and pressure coupling was 2 ps. An isotropic pressure coupling was used in the simulation during equilibration steps. 2.5 ns canonical ensemble (NVT) simulations and 2.5 ns isothermal-isobaric (NPT) simulations were run as an equilibration step, and 10 ns box deformation simulations were performed after the equilibration step. In box deformation simulations, the LAMMPS command "fix deform" was used with the "erate" option to change the dimension of the box at a constant rate every step in order to set the overall box deformation in X axis to be 2 times of the original size in 10 ns of deformation simulations. During the box deformation step, Y, Z directions were coupled with 1 atm Parrinello-Rahman barostat with a damping parameter of 2 ps. In both equilibration and deformation steps, Coulombic interactions were treated with particle-particle particle-mesh (PPPM) method[23] with $\epsilon = 2.5$. A 1.6 nm cutoff distance was used for the short-range electrostatics and van der Waals interactions. The constraint algorithm SHAKE was used to constrain the MARTINI polarizable water dummy bonds[24,25] (For details of MARTINI polarizable water model, see Ref[12]). To account for the 1-3 exclusions inside the MARTINI polarizable water bead, we

modified the "special_bonds" command in LAMMPS so that interactions that were excluded in our model are not calculated, instead of being multiplied by a factor of zero, which would cause a division by zero if the dummy particles inside the CG polarizable water overlaps.

Analysis Methods

Static structure factor

The static structure factor quantifies the spatial correlation of chitosan beads in the polymer network structure over a distance (2π/q). The peak in low-q regime of the static structure factor marks the long range order of the polymer assembly in the system. The static structure factor is related to the radial distribution function g(r) by a Fourier transformation, given by

$$S(q) = 1 + \rho \int_V d\mathbf{r} e^{-i\mathbf{qr}}(g(r) - 1) \tag{2}$$

where g(r) is the radial distribution function from all chitosan beads to all chitosan beads.

Elastic modulus analysis

Elastic moduli of chitosan hydrogel systems were measured by fitting the stress-strain curves during box deformation. Standard error of the fitted elastic modulus is computed from the covariance matrix obtained when fitting the stress-strain curves. In LAMMPS, the "fix deform" command was used to deform the simulation box with a constant strain rate. The measured stress-strain curves were then fitted with a linear function at the zero strain point to calculate the elastic modulus as the slope of the stress-strain curve (Figure S3).

Percolation analysis

Percolation analysis was performed to quantify the connectivity of the chitosan hydrogel network structure through the simulation box. Any two chitosan CG beads within 5.5Å

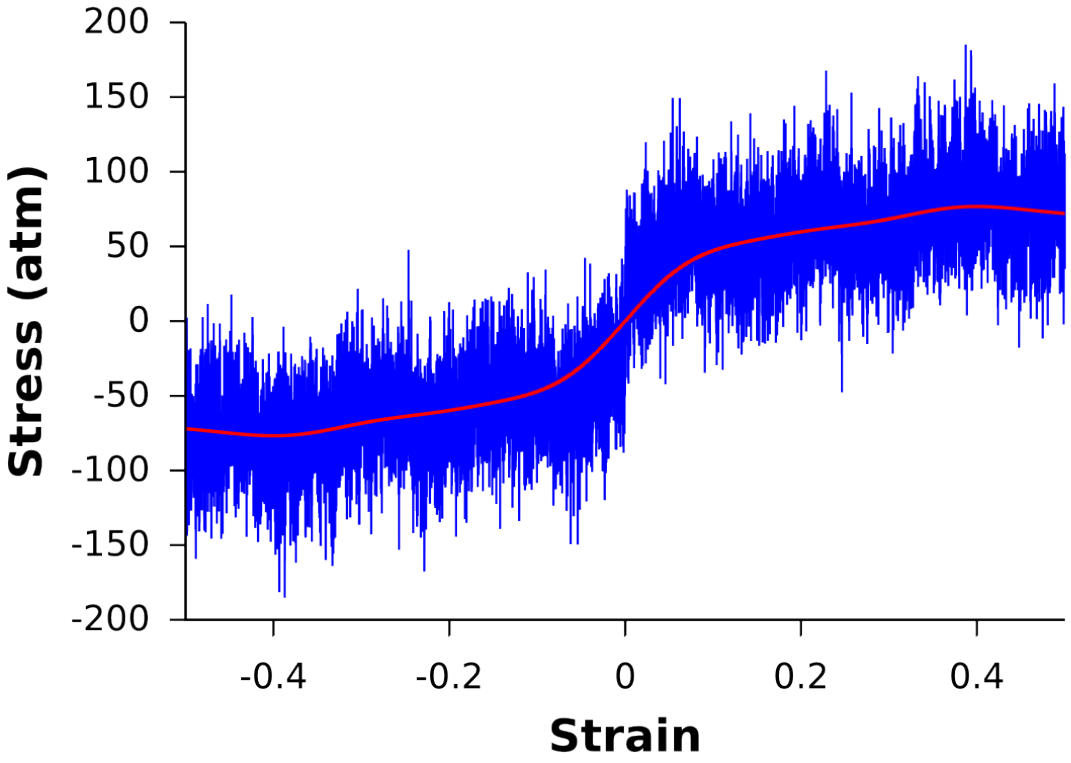

Figure S3: Stress-strain curve (blue) of the chitosan hydrogel system with a water content of 91.1% and a pH greater than 10.5. Red curve is a schematic smoothed stress-strain curve using a Gaussian kernel. The curve in negative strain region is mirrored from positive strain region for fitting purpose.

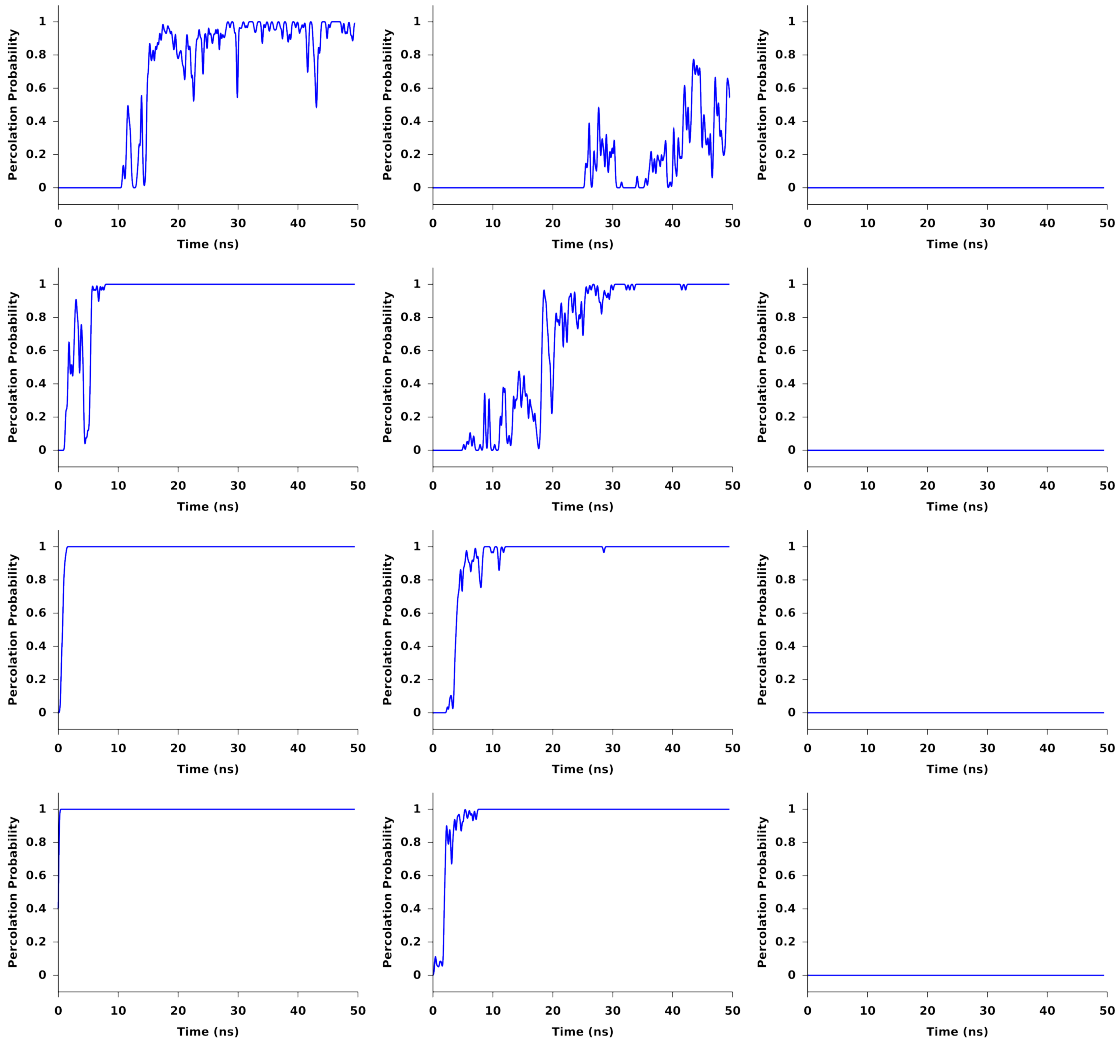

Figure S4: Percolation time series of the chitosan hydrogel network with different pH (a,d,g,j: >10.5; b,e,h,k: 6.5; c,f,i,l: <2.5) and water contents (a,b,c: 95.4%; d,e,f: 91.1%; g,h,i: 86.4%; j,k,l: 82.3%).

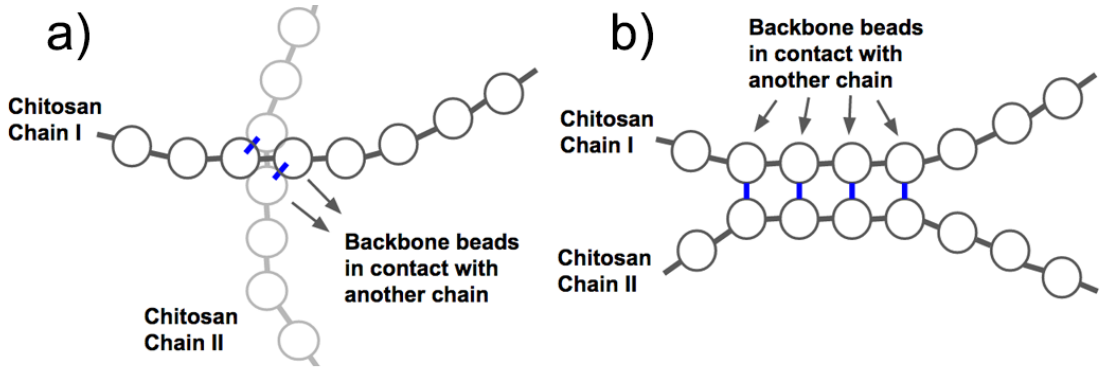

Figure S5: Physical crosslinking pattern schematic illustrations. (a) Perpendicular crosslinking between two chitosan polymer chains; (b) Parallel crosslinking between two chitosan polymer chains.

(which includes the first RDF peak from all chitosan beads to all chitosan beads) were considered connected, and connected polymer chains were defined as percolated if they met both the following conditions: 1) the polymer chains must span the entire box; 2) the polymer chains must connect to themselves through the periodic boundary in all directions. The percolation probability is calculated by sampling the fraction of percolated time every 1ns. The percolation lifetime was calculated by fitting the time series of percolation probability with a sigmoidal curve marking the transition between percolated and un-percolated states.

Crosslinking Pattern Analysis

To characterize the crosslinking pattern of a chitosan hydrogel network, we calculated the polymer chain crosslinking angle cosine ($\cos(\theta)$). The $\cos(\theta)$ ranges from 0 to 1, where 0 means completely perpendicular and 1 means completely parallel. The crosslinking orientation between chitosan polymer chains was calculated from adjacent crosslinking chitosan monomers. The cutoff distance between chitosan monomers is 7.5Å, which includes the first peak of the B2-B2 (backbone bead to backbone bead) radial distribution function. We defined all chitosan monomers within a distance of B2-B2 beads of 7.5Å to be in contact, and a pair of monomers in contact with a crosslinking angle $\cos(\theta)$ over 0.8 was counted as parallel contacts. We then summed up all parallel contacts within the chitosan polymer network to

quantify the amount of parallel crosslinking in the system.

Crosslinking Energy Definition

Crosslinking energy is defined as the sum of interaction potentials between two adjacent chitosan monomer units. For each chitosan monomer, we find all chitosan beads in other chains within its 7.5Å (including first peak of radial distribution function from all B2 beads to all B2 beads) and calculate the sum of all non-bonded interactions between the chitosan monomer and all other chitosan beads.

Pore Size Distribution

Pore size distribution (PSD) histograms are calculated with Zeo++ software.[26] The software uses a number of Monte Carlo samples per unit cell to probe the distribution of pore sizes. The command "network" was used with both *chan_radius* and *probe_radius* set to 1.0 Å, where *chan_radius* is the radius of a probe used to determine accessibility of the pore. *probe_radius* is the radius of a probe used in Monte Carlo sampling. The number of Monte Carlo sampling per atom is set to 5000. To display PSD histograms and compare with static structure factor, we have converted the PSD histogram X axis to be $2\pi/D$, where D is the pore diameter.

References

(1) Uusitalo, J. J.; Ingolfsson, H. I.; Akhshi, P.; Tieleman, D. P.; Marrink, S. J. Martini coarse-grained force field: extension to DNA. *J. Chem. Theory Comput.* **2015**, *11*, 3932–3945.

(2) Brugnerotto, J.; Desbrières, J.; Roberts, G.; Rinaudo, M. Characterization of chitosan by steric exclusion chromatography. *Polymer* **2001**, *42*, 09921–09927.

(3) Schatz, C.; Viton, C.; Delair, T.; Pichot, C.; Domard, A. Typical physicochemical behaviors of chitosan in aqueous solution. *Biomacromolecules* **2003**, *4*, 641–648.

(4) Lamarque, G.; Lucas, J. M.; Viton, C.; Domard, A. Physicochemical behavior of homogeneous series of acetylated chitosans in aqueous solution: Role of various structural parameters. *Biomacromolecules* **2005**, *6*, 131–142.

(5) Brugnerotto, J., Desbrieres, J., Heux, L., Mazeau, K. and Rinaudo, M. Overview on structural characterization of chitosan molecules in relation with their behaviour in solution. *Macromol. Symp* **2001**, *168*, 1–20.

(6) Pol-Fachin, L.; Rusu, V. H.; Verli, H.; Lins, R. D. GROMOS 53A6 GLYC, an improved GROMOS force field for hexopyranose-based carbohydrates. *J. Chem. Theory Comput.* **2012**, *8*, 4681–4690.

(7) Yui, T.; Imada, K.; Okuyama, K.; Obata, Y.; Suzuki, K.; Ogawa, K. Molecular and crystal structure of the anhydrous form of chitosan. *Macromolecules* **1994**, *27*, 7601–7605.

(8) Ogawa, K.; Yui, T.; Okuyama, K. Three D structures of chitosan. *Int. J. Biol. Macromol.* **2004**, *34*, 1–8.

(9) Okuyama, K.; Noguchi, K.; Kanenari, M.; Egawa, T.; Osawa, K.; Ogawa, K. Structural diversity of chitosan and its complexes. *Carbohydr. Polym.* **2000**, *41*, 237–248.

(10) Okuyama, K.; Noguchi, K.; Miyazawa, T.; Yui, T.; Ogawa, K. Molecular and crystal structure of hydrated chitosan. *Macromolecules* **1997**, *30*, 5849–5855.

(11) Lertworasirikul, A.; Yokoyama, S.; Noguchi, K.; Ogawa, K.; Okuyama, K. Molecular and crystal structures of chitosan/HI type I salt determined by X-ray fiber diffraction. *Carbohydr. Res.* **2004**, *339*, 825–833.

(12) Yesylevskyy, S. O.; Schäfer, L. V.; Sengupta, D.; Marrink, S. J. Polarizable water model for the coarse-grained MARTINI force field. *PLoS Comput. Biol.* **2010**, *6*, 1–17.

(13) Hockney, R. W.; Goel, S. P.; Eastwood, J. W. Quiet high-resolution computer models of a plasma. *J. Comput. Phys.* **1974**, *14*, 148–158.

(14) Berendsen, H. J. C.; Postma, J. P. M.; van Gunsteren, W. F.; DiNola, a.; Haak, J. R. Molecular dynamics with coupling to an external bath. *J. Chem. Phys.* **1984**, *81*, 3684–3690.

(15) Sperb, R.; Tironi, I. G.; Tironi, I. G.; Sperb, R.; Smith, P. E.; Smith, P. E.; Gunsteren, W. F. V.; Gunsteren, W. F. V. A generalized reaction field method for molecular dynamics simulations. *J. Chem. Phys.* **1995**, *102*, 5451–5459.

(16) Nosé, S. A unified formulation of the constant temperature molecular dynamics methods. *J. Chem. Phys.* **1984**, *81*, 511.

(17) Hoover, W. G. Canonical dynamics: Equilibrium phase-space distributions. *Phys. Rev. A* **1985**, *31*, 1695–1697.

(18) Parinello, M.; Rahman, A. Polymorphic transitions in single crystals: A new molecular dynamics method. *J. Appl. Phys.* **1981**, *52*, 7182–7190.

(19) Darden, T.; York, D.; Pedersen, L. Particle mesh Ewald: An Nlog(N) method for Ewald sums in large systems. *J. Chem. Phys.* **1993**, *98*, 10089.

(20) Essmann, U.; Perera, L.; Berkowitz, M. L.; Darden, T.; Lee, H.; Pedersen, L. G. A smooth particle mesh Ewald method. *J. Chem. Phys.* **1995**, *103*, 8577–8593.

(21) Hess, B.; Bekker, H.; Berendsen, H. J. C.; Fraaije, J. G. E. M. LINCS: A linear constraint solver for molecular simulations. *J. Comput. Chem.* **1997**, *18*, 1463–1472.

(22) Swope, W. C. A computer simulation method for the calculation of equilibrium constants for the formation of physical clusters of molecules: Application to small water clusters. *J. Chem. Phys.* **1982**, *76*, 637.

(23) Hockney, R. W.; Eastwood, J. W. *SIAM Rev.*; CRC Press, 1983; Vol. 25; pp 425–426.

(24) Ryckaert, J. P.; Ciccotti, G.; Berendsen, H. J. C. Numerical integration of the cartesian equations of motion of a system with constraints: molecular dynamics of n-alkanes. *J. Comput. Phys.* **1977**, *23*, 327–341.

(25) Andersen, H. C. Rattle: A "velocity" version of the shake algorithm for molecular dynamics calculations. *J. Comput. Phys.* **1983**, *52*, 24–34.

(26) Willems, T. F.; Rycroft, C. H.; Kazi, M.; Meza, J. C.; Haranczyk, M. Algorithms and tools for high-throughput geometry-based analysis of crystalline porous materials. *Microporous Mesoporous Mater.* **2012**, *149*, 134–141.